Lyotropic Mesophases of Poly(ethylene oxide)-*b*-poly(butadiene) Diblock Copolymers and Their Cross-Linking To Generate Ordered Gels

H.-P. Hentze,* E. Krämer, B. Berton, S. Förster, and M. Antonietti

Max-Planck-Institut für Kolloid- und Grenzflächenforschung, Kantstrasse 55, D-14513 Teltow-Seehof, Germany

M. Dreja

Institut für Physikalische Chemie der Universität zu Köln, Luxemburger Str. 116, D-50939 Köln, Germany

Received March 18, 1999; Revised Manuscript Received June 28, 1999

ABSTRACT: This study reports the lyotropic phase behavior of two poly(ethylene oxide)-*b*-poly(butadiene) diblock copolymers and their cross-linking in the mesophase under retention of the mesoscopic order. The lyotropic phase behavior in water was characterized by polarized light microscopy and small-angle X-ray scattering (SAXS) in the concentration range from 0 to 100 wt % and in a temperature range between 20 and 100 °C. Depending on polymer composition and concentration micellar, hexagonal, lamellar, and cubic phases are found. Their ranges as well as pronounced coexisting phase regions were determined. Several of these mesophases were cross-linked via γ-irradiation to form mesostructured hydrogels. It is shown that the cross-linked polymer gel essentially maintains the parental lyotropic order, as proven by SAXS, polarized light microscopy, and transmission electron microscopy (TEM). TEM enables imaging of the polymer gel structure and thereby the visualization of the liquid-crystalline mesophase morphologies in themselves. The lyotropic mesophases as well as the lyotropic gels were used as templates for the synthesis of mesoporous silica, which is expected to give a negative solid copy of the ordered soft matter structure. The influence of the different templates on the silica structure formation is discussed.

I. Introduction

Amphiphilic block copolymers (ABC's) consist of at least two polymer blocks with different composition and cohesion energies (e.g., hydrophilic, hydrophobic) that are covalently linked. As with all amphiphiles and block copolymers, amphiphilic block copolymers phase-separate on a mesoscopic length scale which leads to a manifold phase behavior.[1] This structure formation occurs in the bulk phase as well as in selective solvents.

It is well-known that the aggregation behavior of block copolymers in the bulk phase depends on the degree of polymerization N, the volume fractions f of the polymer blocks, and the interaction parameter χ between the blocks.[2,3] Formation of mesophases in the bulk phase can be described by universal phase diagrams as a function of these parameters.[4]

Dilute solutions of amphiphilic block copolymers in selective solvents have also been well studied. In this case, amphiphilic block copolymers aggregate into micelles, the aggregation number of which is directly related to the molecular geometry of the amphiphile, which was recently described by a universal relation.[5] Besides spherical micelles, other aggregate structures, such as wormlike micelles, toroids, or vesicles, were also described.[6−8] Similar to their low molecular weight counterparts, a particular amphiphilic block copolymer usually does not realize all different aggregation structures, but the morphology responds to the molecular geometry, the concentration of the amphiphile, and the solvent.

Another analogy between low molecular weight surfactants and amphiphilic block copolymers is the formation of lyotropic mesophases in the concentration range between micellar solutions and the bulk phase. The aggregation behavior in this intermediate concentration range is by far not that well investigated and understood. Pioneering work on Pluronics, a certain class of poly(ethylene oxide)-*b*-poly(propylene oxide) diblock and triblock copolymers,[9,10] showed that the position of the phase regions in the binary phase diagrams is nearly independent of the molecular weight of the block copolymer and depends strongly on the block length ratio.

Here we report the lyotropic phase behavior of poly(ethylene oxide)-*b*-poly(butadiene) block copolymers, their ability to form self-organized assemblies, and their cross-linking to generate covalently linked, mesostructured polymer gels with preservation of the original structure. Lyotropic mesophases and their polymerized gels were characterized by polarized light optical microscopy (POM), small-angle X-ray scattering (SAXS), and transmission electron microscopy (TEM). Ultramicrotomy of the polymer gels allows the direct imaging of the phase morphologies by electron microscopy.

Another motivation for the examination of the lyotropic mesophases of ABC's lies in the increasing utilization of the principle of self-organization in modern materials science. Self-organized media, such as microemulsions,[11−14] vesicular solutions,[15,16] bicontinuous microemulsions,[17−19] and lyotropic mesophases,[20] have turned out to be very useful templates for the colloidal structure design of nanomaterials. In these procedures, the rather fragile self-assembled structures are turned into solid and permanent stable mesostructured materials. For all these techniques, polymeric amphiphiles are promising because they usually show very low critical micelle concentrations (cmc), slow exchange dynamics, and kinetically more stable aggregate structures which makes them more robust templates.[20] Another versatile advantage of amphiphilic block copolymers is that their

10.1021/ma9904058 CCC: $18.00
Published on Web 07/30/1999

Table 1. Characteristics of the PEO-*b*-PB Copolymers[a]

sample	N(PEO)	N(PB)	M_w/M_n	f_{PEO}
P1	125	155	1.02	0.55
P2	202	360	1.06	0.64

[a] N(PEO) = degree of polymerization of the PEO block (from ^{1}H NMR data[30]); N(PB) = degree of polymerization of the PB block (from GPC data[30]); M_w/M_n = molecular weight distribution calculated from GPC data[30] and f_{PEO} is the volume fraction of the PEO block.

lyotropic phase behavior as well as their mesoscopic dimensions can be easily adjusted by changing the block lengths, as for example in the templating of mesoporous silica.[21−24]

Lyotropically ordered gels in this sense would represent templates with infinite kinetic stability. Most trials to form lyotropic ordered gels by polymerization processes of inert monomers in surfactant assemblies however have failed, which is due to the entropic influence of the growing polymer chain on the ordered phase. O'Brien and also Gin reported on the preservation of order in some special polymerizable surfactants.[25,26] The γ-ray polymerization of lyotropic mesophases of low molecular weight polymerizable surfactants was also carried out.[27] Compared to low molecular weight materials, γ-ray cross-linking of polybutadiene-containing ABC's promises a number of advantages.[6,28,29] Besides improved kinetic stability of the polymeric template, the much higher number of polymerizable units per molecule ensures homogeneous cross-linking already at very low conversions. In this way any changes of the parental structure can be suppressed already during the very early stages of reaction. The resulting cross-linked mesophases were used as templates for silica casting. The resulting silica morphologies were compared to those obtained from templating with the primary, non-cross-linked mesophases under otherwise unchanged conditions.

II. Experimental Part

II.1. Materials. Poly(ethylene oxide)-*b*-poly(butadiene) diblock copolymers were synthesized by anionic polymerization according to literature procedures.[30] The molecular properties of the polymers P1 and P2 are summarized in Table 1. Deionized water (Milli-Q) was used for the preparation of the aqueous polymer solutions.

II.2. Preparation and Polymerization of Lyotropic Mesophases. Lyotropic mesophases of amphiphilic block copolymers were prepared by mixing the polymer and deionized water in 5 mL test tubes. After homogenization by intense mechanical stirring, the sealed samples were equilibrated at 60 °C for 24 h and stored at 25 °C for another 48 h. The polymerization of the samples was carried out using a ^{60}Co γ-irradiation source (dose rate: 55.67 krad/h = 0.5567 kGy/h). The overall radiation dose for all samples was 13.15 Mrad = 131.5 kGy (1 rad = 0.01 J/kg = 0.01 Gy).

II.3. Synthesis of Mesoporous Silica. The synthesis of mesoporous silica within the non-cross-linked phase was performed as described in the literature.[31] For the synthesis of silica within the polymer gel, the silica precursor TMOS (tetramethoxysilane) was prehydrolyzed. Therefore, a mixture of 6 g of TMOS and 3 g of HCl (pH 2) was stirred at 50 °C until it became a single-phase silicic acid solution. A slice of the polymer gel (1 g) was placed within the silicic acid for 15 min. After removing the swollen slice from this solution, the polycondensation of the silicic acid occurred by heating the polymer gel for 6 h at 60 °C in a drying oven. Removal of organic matter from the silica matrix was done by heating the hybrid gel in a quartz glass tube for 4 h under nitrogen at 500 °C, followed by 12 h under oxygen.

II.4. Analytical Methods. *Optical Microscopy.* The lyotropic phase behavior of the amphiphilic block copolymers was studied by polarized light optical microscopy (POM) using a Leica DM R optical microscope and a Linkam THM 600/S hotstage. To investigate the phase diagrams, polymer solutions were prepared in 2−5 wt % intervals. The lyotropic mixtures were heated between two glass slides from room temperature (20 °C) up to 100 °C using various constant heating rates from 2.0 to 0.1 °C/min. The occurrence of phase separations was checked by phase contrast optical microscopy.

Small-Angle X-ray Scattering. Small-angle X-ray scattering (SAXS) measurements were performed using a camera constructed at the Max-Planck-Institut of Colloids & Interfaces. Cu Kα X-rays were generated by a rotating anode (Nonius, FR591). The lyotropic solutions were sealed in fine-glass capillary tubes (1 mm in diameter). The accessible s range is $0.01\ \text{nm}^{-1} < s < 0.30\ \text{nm}^{-1}$, where the scattering vector is defined as $s = 2/\lambda \sin\theta$ with 2θ being the angle between the incident and the scattered light.

Transmission Electron Microscopy. The polymerized gels were examined using transmission electron microscopy (TEM). For this purpose the gels were dried using a critical-point apparatus (BAL-TEC CPD 030) after a stepwise exchange of water for acetone followed by a subsequent solvent exchange to supercritical CO_2. The dried gels were embedded in a polyepoxide matrix for ultramicrotoming using a Leica Ultracut UCT ultramicrotom. The cut sections had a thickness of about 30−50 nm and were examined with a Zeiss EM 912 OMEGA transmission electron microscope.

III. Results and Discussion

Lyotropic Phase Behavior. Figure 1a,b gives a schematic phase assignment of the two polymers P1 and P2, as revealed by POM.

Polymer P1 forms clear and isotropic micellar solutions up to 25 wt % at temperatures between 20 and 77 °C. Above 77 °C demixing occurrs, as is typical for nonionic surfactants of the C_iE_j-type with low poly(ethylene oxide) content due to reduced hydration of the hydrophilic block (cloud point).[33] In contrast to low molecular weight surfactants, no macroscopic phase separation is observed, as the viscosity of the mesophases is high. Phase contrast microscopy clearly confirms the demixing into domains of several tenths of micrometers in size. The cmc appears to be very low. Already at concentrations of 0.1 wt % wormlike micelles were detected at 25 °C by dynamic light scattering and atomic force microscopy (AFM).[7] At higher weight fractions (>25 wt %), slightly opaque and optically anisotropic lyotropic mesostructures are observed. A hexagonal phase (H_I) occurs between 25 and 57 wt % which shows a weak fan texture (Figure 2a). The corresponsing SAXS pattern of a sample with 50 wt % polymer P1 shows no fewer than five peaks, which underlines the high degree of order of the mesophase (Figure 3a). The characteristic length of the hexagonal phase, given by the d spacing calculated from the first peak, is 44 nm ($s = 2/\lambda \sin\theta = 1/d$).

At concentrations above 66 wt %, a lamellar mesophase (L_α) is observed which persists until a lamellar bulk phase at 100 wt % block copolymer is reached. The typical POM texture of this lamellar mesophase is depicted in Figure 2a. The SAXS pattern of a sample with 70 wt % ABC shows no fewer than nine equidistant peaks (Figure 3b), again indicating the very high degree of order of these polymeric lyotropic mesophases. The d spacing of the lamellar structure of P1 at 70 wt % is 31 nm. Both POM and SAXS indicate that a two-phase coexistence region occurs between the hexagonal and

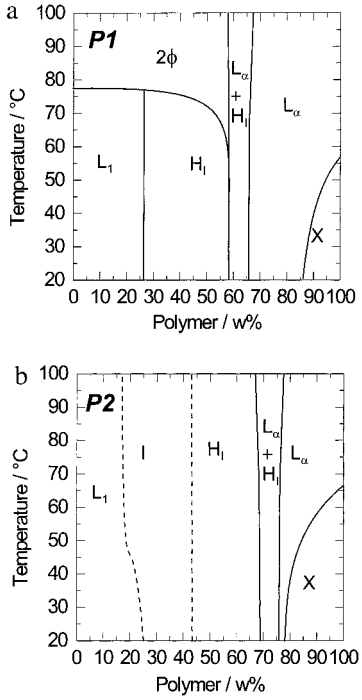

Figure 1. Binary phase diagrams (composition versus temperature) of the PEO-*b*-PB block copolymers (a) P1 and (b) P2 in water as revealed by polarized light optical microscopy.

the lamellar phase, which shows that even after longer equilibration times, there is no macroscopic demixing. The detailed discussion of the structure of this coexistence region will be given in context with the TEM results. Analogous to poly(ethylene oxide)-*b*-poly(ethylethylene) block copolymers,[32] a semicrystalline phase (X) is formed at low temperatures and high concentrations (>86 wt %) where a liquid lamellar mesophase and small PEO crystallites coexist, indicated by POM, showing optical textures of PEO spherolites.

The phase diagram of P2 with its higher relative PEO content differs from that of P1. Up to 25 wt % a micellar solution is formed. A hexagonal phase occurs at 45−75 wt %. Between the micellar and the hexagonal phase, a cubic phase (I) is formed around 40 wt % polymer, which however is barely defined by POM, as indicated by the dashed lines. For a better determination of the phase range, more detailed rheological or SAXS investigations would be necessary. At concentrations higher than 85 wt % a lamellar mesophase is found. Both hexagonal and lamellar mesophases show POM textures similar to the ones shown in Figure 2, and SAXS supports these classifications. By showing a superimposition of both scattering patterns, SAXS measurements also hint at a coexistence phase region between the H_I and the L_α phases, which demand further investigations in the concentration range between 60 and 75 wt %. The phase region of the semicrystalline phase (X) is even larger than that of P1, due to the higher tendency of the longer PEO block to crystallize.

To sum up, both phase diagrams go well with the systematic trends seen for C_iE_j-type surfactants.[33] A direct comparison of both PEO-*b*-PB phase diagrams shows that the polymer with the higher volume fraction of polar chain, P2 ($f_{PEO} = 0.64$ for polymer P2 as compared to $f_{PEO} = 0.55$ for polymer P1), tends to form aggregates with a higher curvature toward water, resulting in a shift of phase regions toward higher concentrations as compared to the case of P1. The higher

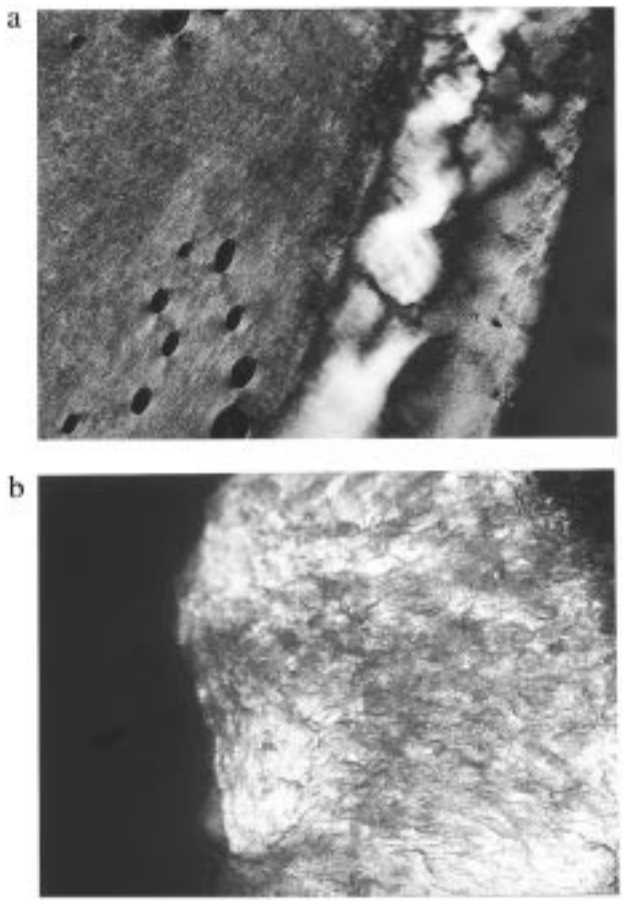

Figure 2. (a) A contact preparation of the lamellar phase (90 wt % P1) with water. The concentration of the polymer decreases from the left to the right. The texture of the hexagonal phase occurs between the texture of the lamellar phase (left) and the isotropic micellar phase (dark region, right). (b) The texture of the cross-linked hexagonal hydrogel (50 wt % P1).

amount of PEO also suppresses the occurrence of a high-temperature miscibility gap.

***γ*-ray Cross-Linking of Lyotropic Mesophases.** *γ*-ray cross-linking was performed within the cubic, hexagonal, and lamellar phases and the coexistence regions of PEO-*b*-PB block copolymers. After *γ*-irradiation with a dose of 13.15 Mrad, all samples turned into solid, mechanically stable and elastic hydrogels. After irradiation, all materials were completely cross-linked, as no unreacted polymer could be isolated by Soxhlet extraction using water or acetone as solvents. Within all samples, the water-swollen poly(ethylene oxide) blocks form the continuous phase. Addition of water after cross-linking leads to swelling but not to a dissolution of the gel structure. This is an indirect proof that cross-linking occurs not only in the polybutadiene units but also in the polyether block, as was reported for PEO homopolymer solutions[34,35] for the synthesis of drug release systems.[36] A reexamination of the samples after cross-linking by POM showed the preservation of optical textures (Figure 2b). Even after drying, the textures of the gels are not changed, indicating the retention and immobilization of the lyotropically organized morphology.

SAXS measurements of the cross-linked hydrogel show essentially the same peak sequences and peak profiles, but all peaks are slightly shifted to higher *s* values (Figure 3a,b). This means that the cross-linking

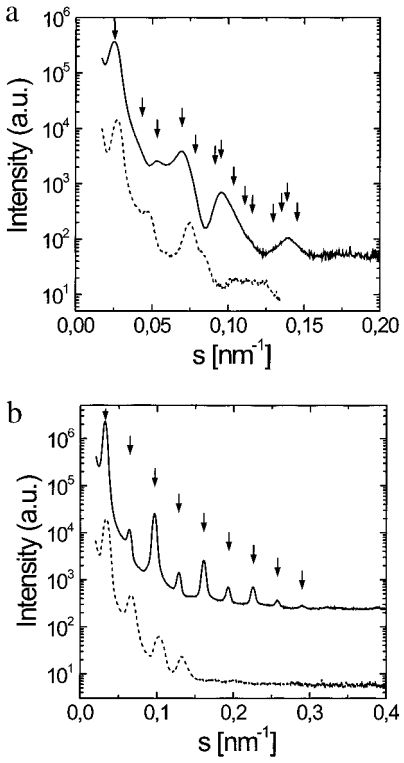

Figure 3. SAXS diffractograms of (a) the hexagonal (50 wt % P1) and (b) the lamellar (70 wt % P1) mesophase of polymer P1 in water, prior to (solid line) and after (dashed line) cross-linking. Arrows mark the expected peak positions for the indicated morphologies. (The spacing ratios of the expected peaks are 1:√3:√4:√7:√9:√12:√13... for the hexagonal and 1:2:3:4:5:6:7... for the lamellar phase.)

effects a decrease of *d* spacings on the order of 5−10%. Thin sections of critical point dried polymer gels were used for TEM studies to visualize the morphologies of the lyotropic organized gel structures. TEM micrographs of the critical point dried, cross-linked lyotropic mesophases of polymer P1 are depicted in Figure 4a−c.

Figure 4a shows the TEM micrograph of the cross-linked hexagonal phase at 50 wt % P1. The lengths of the sectioned cylinders vary strongly, due to the different orientation of the cylinders with respect to the cut direction. The radius of the cylinders is constant at about 10 nm. The long period of the cross-linked and dried hexagonal phase is determined to be about 40 nm, which corresponds well to the primary, non-cross-linked mesophase. γ-Irradiation of a mesophase containing 70 wt % P1 results in a lamellar hydrogel as shown in Figure 4c. The distances between the single lamellae seem to vary strongly, which is again affected by the different orientation of the aggregates with respect to the cut direction.

Between the hexagonal and the lamellar mesophase, a coexistence region was observed. The corresponding cross-linked hydrogel shown in Figure 4b allows direct visualization of the mesophase structure in the coexistence range at 60 wt % P1 in water. Both cylinders and lamellae are observed in the direct neighborhood of each other, indicating a possible transition between these two mesoscopic geometries. Even the dynamic zipperlike mechanism which turns the cylinders into lamellae was frozen by cross-linking in some parts of the sample and can therefore statically be visualized.[7]

The TEM micrographs in Figure 5a−d represent the results of γ-ray cross-linking of some of the mesophases

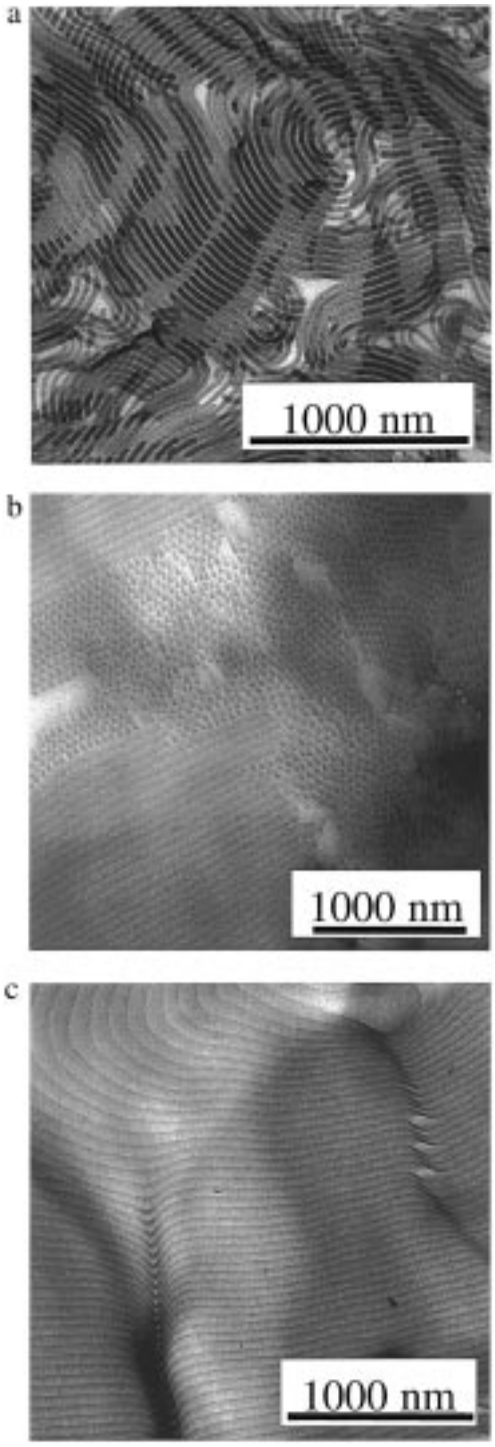

Figure 4. TEM micrographs of cross-linked mesophases of polymer P1. (a) A dense packing of cylinders is obtained from cross-linking of the hexagonal (H_I) phase (cross-linked at 50 wt % P1). (b) Gel structure in the transition range (cross-linked at 60 wt % P1); coexistence of lamellae and cylinders. (c) Morphology of the cross-linked lamellar (L_α) mesophase (cross-linked at 70 wt % P1).

formed by polymer P2. In accordance with the higher molecular weight and the longer contour lengths of the blocks, the mesophases and polymer gels of polymer P2 show generally larger characteristic lengths. Due to the different block length ratio, a cubic phase is also accessible which results in a bcc ordered polymer gel after γ-ray cross-linking as shown in Figure 5a (40 wt % P2). The morphologies of the hexagonal and lamellar ordered gels are depicted in Figure 5b,d (50 and 80

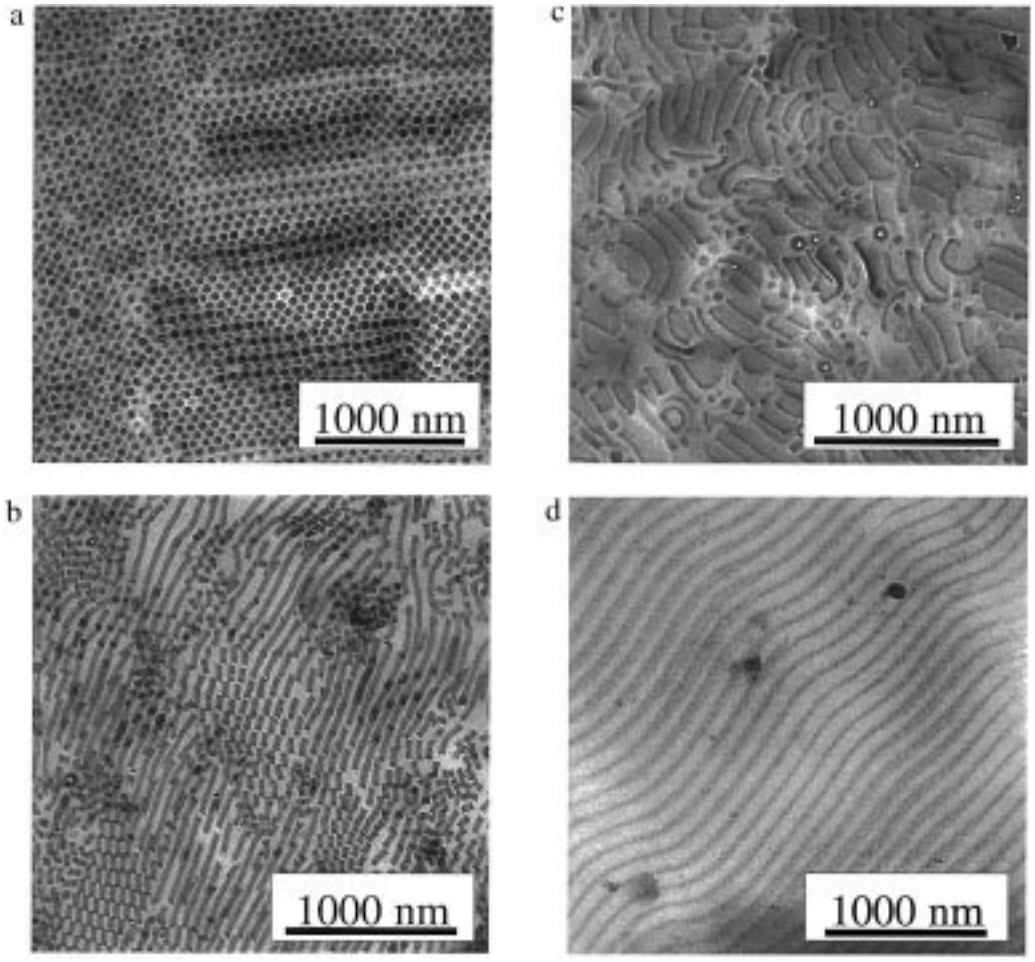

Figure 5. TEM micrographs of cross-linked mesophases of polymer P2. (a) Cubic (I) gel gel structure (cross-linked at 40 wt % P2). (b) Cylinders of the hexagonal (H_I) phase (cross-linked at 50 wt % P2). (c) Transition range with platelets, vesicles, and single lamellae (cross-linked at 60 wt % P2). (d) Cross-linked lamellar (L_α) mesophase (cross-linked at 80 wt % P2).

Table 2. Swelling of Cross-Linked and Dried Gels with Water and Toluene[a]

	weight increase, %	
compound	in water	in toluene
P1 (H_I, 50 wt %)	131	72
P1 (L_α, 70 wt %)	88	79

[a] Weight increase of critical point dried, hexagonal and lamellar ordered gels of polymer P1 by swelling with water and toluene.

wt % P2) whereas Figure 5c (70 wt % P2) again illustrates the morphology of the mesophase in the coexistence range between the hexagonal and the lamellar mesophases. Here the cylinders coexist with different low-curvature, layerlike structures, such as platelets, vesicles, and single lamellae.

All cross-linked and dried PEO-*b*-PB gels were swellable in polar and nonpolar solvents, such as water and toluene (Table 2). Swelling with these solvents as well as changes in temperature had no influence on the optical textures; only the intensity of birefringence increases by swelling with toluene. This underlines that the internal order is irreversibly fixed by cross-linking of both the hydrophilic and hydrophobic domains.

Lyotropic Ordered Polymer Gels as Templates for Mesoporous Silica. Recently, the use of lyotropic mesophases of amphiphilic block copolymers for the synthesis of mesoporous silica was reported.[21−24] The variation of block lengths and concentrations allows the adjustment of pore sizes, porosities, and morphologies in a range that clearly exceeded those of classical MCM-type materials. By SAXS measurements, it was demonstrated that the generated silica matrix adopts the same order as the lyotropic template, whereas the long period was slightly decreased, as to be expected for a polycondensation reaction.

Up to now, a direct comparison of the template and the silica morphology by imaging was not possible. This is enabled by the γ-ray cross-linking of the block copolymer templates. Silica templating can be conducted in both cross-linked and non-cross-linked lyotropic phases. The resulting morphologies can be compared with the cross-linked template and should give direct proof for the retention of morphology.

The synthesis of mesoporous silica within the non-cross-linked hexagonal phase of polymer P1 (50 wt %) was carried out under acidic conditions using the silica precursor tetramethoxysilane (TMOS) as described in the literature.[31] The polycondensation of this precursor within the cross-linked hexagonal mesophase was performed by maximal swelling of the network with a precondensed 1:1 hydrochloric acid (pH 2)/TMOS mixture, followed by polycondensation at 60 °C and calcination. The TEM micrographs of the calcined and thin-sectioned silica ceramics are shown in Figure 6a,b.

Both silica structures show nearly the same morphology. The characteristic lengths vary slightly as shown by SAXS measurements. Using the non-cross-linked template, the *d* spacing is 31 nm. Templating within

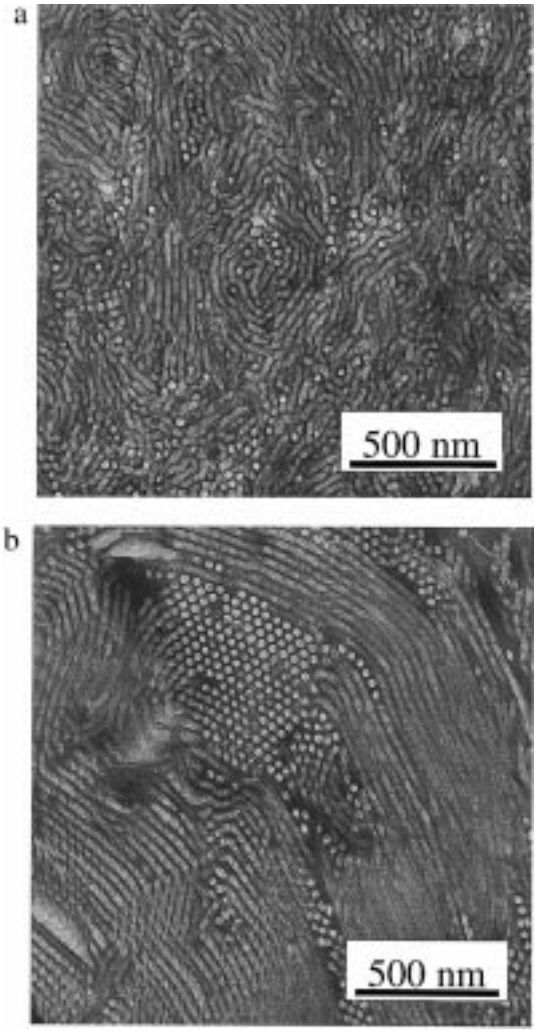

Figure 6. TEM micrographs of mesoporous silica. (a) Silica templated within the non-cross-linked hexagonal (H_I) mesophase of polymer P1 (50 wt % P1). (b) Silica templated within the cross-linked hexagonal phase (cross-linked at 50 wt % P1) after swelling with silicic acid. Both samples show the same hexagonal order.

the cross-linked mesophase results in a *d* spacing of 34 nm. This slight difference results from the different amount of precursor that was used, as a result of the different methods of precursor addition (addition of TMOS/swelling with silicic acid). The TEM micrographs show also a different ratio of length dimensions and a higher degree of order in the case of using the cross-linked template, which might be affected by the different times of equilibrating the lyotropic phases. All in all the morphologies of the templated silica materials and the cross-linked polymer template correspond directly. These results confirm the above statements to structure preservation which were made so far only on the basis of scattering data.

IV. Conclusion and Outlook

γ-ray cross-linking of lyotropic PEO-*b*-PB block copolymer phases enables the synthesis of organic polymer gels under complete retention of the original mesoscopic order. Using this approach, comparably fragile self-organized nanostructures of lyotropic mesophases are turned into temperature- and solvent-insensitive, solid and mechanically stable materials. Morphology and size of the compartments can be controlled by adjusting the polymer concentration and varying the block length of the polymer.

This procedure is interesting from an analytical as well as a synthetic point of view. Considering analysis, imaging the primary aggregate structures using ultramicrotomy and TEM gives new insights in the formation mechanism of lyotropic mesophases. Thereby the structures of the different mesophases in single phase, transition, and coexistence ranges can be directly visualized. A convenient way to generate mesoscopically ordered gels is described, the morphology of which is stable against changes of temperature and concentration, addition of solvents, or even drying. Addition of polar or nonpolar solvents do not change the order of the gels but only the characteristic lengths of the lyotropic ordered materials by the degree of swelling.

Mesoporous silica was synthesized using the novel cross-linked lyotropic block copolymer mesophases as templates. By TEM studies, it was demonstrated that the lyotropic ordered structure is retained during the sol−gel process, even for the non-cross-linked mesophases.

Potential applications of such compartimentized amphiphilic polymer gels lie within the fields of membranes, which are swellable in both hydrophilic and hydrophobic solvents, bioseparation, and controlled drug delivery systems. An advantage of γ-ray cross-linking for the latter application is the possible incorporation of polar and nonpolar drugs without using an additional chemical cross-linking agent.

Acknowledgment. The authors thank C. Göltner for helpful discussions and I. Zenke for technical assistance. M.A. and H.P.H. thank Erich C. for controlled delivery applications. Financial support by the Max-Planck-Society is gratefully acknowledged.

References and Notes

(1) Förster, S.; Antonietti, M. *Adv. Mater.* **1998**, *10*, 195.
(2) Matsen, M. W.; Schick, M. *Macromolecules* **1994**, *27*, 4014.
(3) Vavasour, J. D.; Whitmore, M. D. *Macromolecules* **1992**, *25*, 5477.
(4) Förster, S.; Khandpur, A. K.; Zhao, J.; Bates, F. S.; Hamley, I. W.; Ryan, A. J.; Bras, W. *Macromolecules* **1994**, *27*, 6922.
(5) Förster, S.; Zisenis, M.; Wenz, E.; Antonietti, M. *J. Chem. Phys.* **1996**, *104*, 9956.
(6) Won, Y. Y.; Davis, H. T.; Bates, F. S. *Science* **1999**, *283*, 960.
(7) Förster, S., unpublished results.
(8) Yu, K.; Eisenberg, A. *Macromolecules* **1998**, *31*, 3509.
(9) Wanka, G.; Hoffmann, H.; Ulbricht, W. *Macromolecules* **1994**, *27*, 4145.
(10) Alexandridis, P.; Zhou, D.; Khan, A. *Langmuir* **1996**, *12*, 2690.
(11) Candau, F. In *Polymerization in Organized Media*; Paleos, C. M., Ed.; Gordon Science Publishers: Philadelphia, 1992; p 215.
(12) Full, A. P.; Puig, J. E.; Gron, L. U.; Kaler, E. W.; Minter, J. R.; Mourey, T. H.; Texter, J. *Macromolecules* **1992**, *25*, 5157.
(13) Dreja, M.; Tieke, B. *Langmuir* **1998**, *14*, 800.
(14) Antonietti, M.; Basten, R.; Lohmann, S. *Macromol. Chem. Phys.* **1995**, *196*, 441.
(15) Morgan, J. D.; Johnson, C. A.; Kaler, E. W. *Langmuir* **1997**, *13*, 6447.
(16) Hotz, J.; Meier, W. *Adv. Mater.* **1998**, *10*, 1387.
(17) Palani Raj, W. R.; Sasthav, M.; Cheung, H. M. *Polymer* **1993**, *34*, 3305 and references therein.
(18) Chieng, T. H.; Gan, L. M.; Chew, C. H.; Lee, L.; Ng, S. C.; Pey, K. L.; Grant, D. *Langmuir* **1995**, *11*, 3321 and references therein.
(19) Antonietti, M.; Hentze, H. P. *Colloid Polym. Sci.* **1996**, *274*, 696.
(20) Antonietti, M.; Göltner, C. G.; Hentze, H. P. *Langmuir* **1998**, *14*, 2670.
(21) Göltner, C. G.; Antonietti, M. *Adv. Mater.* **1997**, *9*, 431.

(22) Göltner, C. G.; Henke, S.; Weissenberger, M. C.; Antonietti, M. *Angew. Chem., Int. Ed. Engl.* **1998**, *37*, 613.
(23) Templin, M.; Franck, A.; Duchesne, A.; Leist, H.; Zhang, Y. M.; Ulrich, R.; Schadler, V.; Wiesner, U. *Science* **1997**, *278*, 1795.
(24) Zhao, D. Y.; Feng, J. L.; Huo, Q. S.; Melosh, N.; Fredrickson, G. H.; Chmelka, B. F.; Stucky, G. D. *Science* **1998**, *279*, 548.
(25) Srisiri, W.; Lee, Y. S.; Sisson, T. M.; Bondurant, B.; O'Brien, D. F. *Tetrahedron* **1997**, *53*, 15397.
(26) Gray, D. H.; Hu, S.; Juang, E.; Gin, D. L. *Adv. Mater.* **1998**, *9*, 731.
(27) Pawlowski, D.; Haibel, A.; Tieke, B. *Ber. Bunsen-Ges. Phys. Chem.* **1998**, *102* (12), 1865.
(28) Lipic, P. M.; Bates, F. S.; Hillmyer, M. A. *J. Am. Chem. Soc.* **1998**, *120*, 8963.
(29) Liu, G. J.; Ding, J. F. *Adv. Mater.* **1998**, *10*, 69.
(30) Förster, S.; Krämer, E. *Macromolecules*, in press.
(31) Weissenberger, M. C.; Göltner, C. G.; Antonietti, M. *Ber. Bunsen-Ges. Phys. Chem.* **1997**, *101*, 1679.
(32) Hajduk, D. A.; Kossuth, M. B.; Hillmyer, M. A.; Bates, F. S. *J. Phys. Chem. B* **1998**, *102*, 4269.
(33) Mitchell, D. J.; Tiddy, G. J. T.; Waring, L.; Bostock, T.; McDonald, M. P. *J. Chem. Soc., Faraday Trans. 1* **1983**, *79*, 975.
(34) Charlesby, A.; *Kobunshi (High Polymers)* **1965**, *14*, 156.
(35) King, P.; Warwick, N. US Patent 3 264 202, 1966.
(36) Lambov, N.; Stanchev, D.; Peikov, P.; Belcheva, N.; Stamenova, R.; Tsvetanov, C. B. *Pharmazie* **1995**, *50*, 126.

MA9904058